JOC Article

Di-(*R*,*R*)-1-[10-(1-hydroxy-2,2,2-trifluoroethyl)-9-anthryl]-2,2,2-trifluoroethyl Muconate: A Highly Chiral Cavity for Enantiodiscrimination by NMR

Martina Palomino-Schätzlein, Albert Virgili,* Sergio Gil, and Carlos Jaime

Departament de Química, Universitat Autònoma de Barcelona, 08193 Bellaterra, Barcelona, Spain

albert.virgili@uab.es

Received June 21, 2006

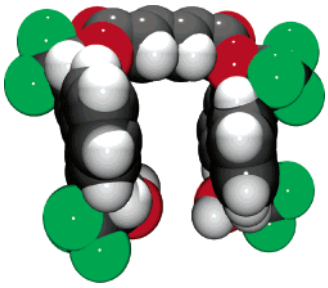

A new chiral molecular tweezer, di-(*R*,*R*)-1-[10-(1-hydroxy-2,2,2-trifluoroethyl)-9-anthryl]-2,2,2-trifluoroethyl muconate **2**, was synthesized in enantiopure form, and its geometry was studied using NMR and molecular mechanics. The effectiveness of **2** as a chiral solvating agent for determining the enantiomeric composition of chiral compounds using NMR was demonstrated, improving the results obtained with other methods. The stoichiometry and the association constant of the resulting diastereomeric complexes were studied, and their geometry was analyzed by NOE and ^{1}H NMR.

Introduction

NMR spectroscopy is one of the most important methods for analyzing chiral molecules. A wide variety of enantiodiscriminating agents have been developed to determine the enantiomeric ratio (er)[1] and/or assignment of absolute configuration.[2]

Chiral solvating agents (CSA) are optically pure compounds that bind in situ to the substrate through noncovalent, intermolecular forces, usually under conditions of fast exchange between the bound and the unbound forms.[3] The associated complexes of a pair of enantiomers with a CSA are diastereomers and are the source of discrimination in the NMR spectrum. Enantiodifferentiation can occur because of different intrinsic spectra of the complexes or because of the different time-averaged solvation environments caused by unequal association constants.

Common CSAs are donor−acceptor compounds that can participate in hydrogen bonds or π interactions. Some chiral solvating agents are host compounds, the most known of which are cyclodextrins[4] and crown ethers.[5] In this case, steric effects are highly significant. Moreover, noncyclic compounds with flexibly sized cavities, which are frequently termed molecular tweezers or clips, proved to be effective as synthetic receptors. This kind of compound is characterized by having two planar, aromatic groups, separated by a semirigid spacer, which enhances the selective binding with aromatic guests by π interactions.[6] Though a large number of molecular tweezers have been developed, only a few examples of chiral molecular tweezers can be found.[7]

(1) Gawlay, R. E. *J. Org. Chem.* **2006**, *71*, 2411−2416.
(2) (a) Wenzel, T. J.; Wilcox, J. D. *Chirality* **2003**, *15*, 256−270. (b) Parker, D. *Chem. Rev.* **1991**, *91*, 1441−1457.
(3) Pirkle, W. H.; Hoover, D. J. *Top. Stereochem.* **1982**, *1*, 263−331.
(4) (a) Kano, K.; Hasegawa, H.; Miyamura, M. *Chirality* **2001**, *13*, 474−482. (b) Kitae, T.; Takashima, H; Kano, K. *Inclusion Phenom.* **1999**, *33*, 345−359.
(5) (a) Bang, H.; Edwards, J. O.; Kim, J.; Lawler, R. G.; Reynolds, K.; Ryan, W. J.; Sweigart, D. A. *J. Chem. Soc., Perkin Trans. 2* **2001**, 1685−1692. (b) Wenzel, T. J.; Thurston, J. E.; Sek, D. C.; Joly, J.-P *Tetrahedron: Asymmetry.* **2001**, *12*, 1125−1130.
(6) Harmata, M. *Acc. Chem. Res.* **2004**, *37*, 862−873.
(7) (a) Mas, T.; Pardo, C.; Salort, F.; Elguero, J.; Torres, M. R. *Eur. J. Org. Chem.* **2004**, 1097−1104. (b) Potluri, V. K.; Maitra, U. *J. Org. Chem.* **2000**, *65*, 7764−7769. (c) Harmata, M.; Barnes, C. L.; Srinivasa R.; Elahmad, S. *J. Am. Chem. Soc.* **1994**, *116*, 8392−8393. (d) Legrand, S.; Luukinen, H.; Isaksson, R.; Kilpeläinen, I.; Lindström, M.; Nicholls, I. A.; Unelius, C. R. *Tetrahedron: Asymmetry* **2005**, *16*, 635−640. (e) Tanaka, K.; Ootani, M.; Toda, F. *Tetrahedron Asymmetry*, **1992**, *3*, 709−712.

10.1021/jo061276d CCC: $33.50
Published on Web 09/21/2006

SCHEME 1. Synthesis of Ester 2

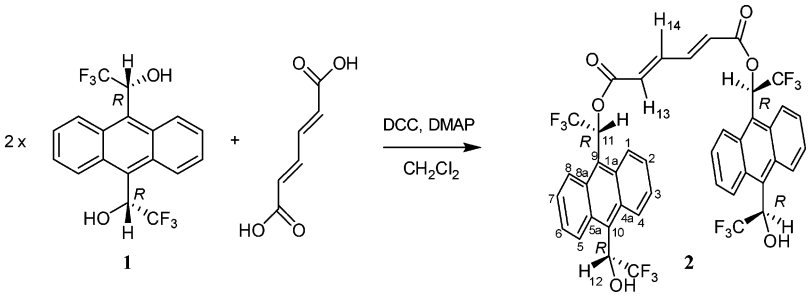

The aim of this work was to develop a chiral molecular tweezer which could be used as a chiral solvating agent. The new compound would be formed by two aromatic chiral molecules, α,α′-(bistrifluoromethyl)-9,10-anthracenedimethanol **1**(ABTE), bonded and separated by a spacer, which would allow a chiral cavity to be formed. α,α′-(Bistrifluoromethyl)-9,10-anthracenedimethanol[8] has been proven to be a highly effective CSA because of the presence of two chiral groups which contain acidic hydroxyl groups that are capable of forming two hydrogen bonds with the substrate at the same time.[9] Similarly, the target molecule will have two chiral hydroxyl groups, and its concave−convex topology will also optimize the interactions with the solute.

First, the enantioselective synthesis of the molecular tweezer will be described and its geometry studied using NMR and molecular mechanics. Next, its enantiodifferentiation capacity as a CSA will be assayed with different racemic mixtures and compared with other efficient CSAs. Finally, the geometry of some diastereomeric complexes will be studied in more detail to understand the enantiodiscrimination mechanism.

Results and Discussion

Synthesis and Structural Analysis. The spacer molecule should have a length of 6−8 carbon atoms, to set a distance between the pincers of the tweezer of about 7 Å, which is ideal for including a single aromatic guest.[10] In addition, the spacer should be a moderately rigid molecule, to hold the pincers in an open conformation so they can be adapted to the substrate to be recognized. Commercial muconic acid (*trans*,*trans*-2,4-hexadienedioic acid) matches these requisites and can be bound to ABTE by an esterification reaction.

R,*R*-ABTE was prepared in enantiopure form by the established procedure[11] and its enantiomeric composition (98%) was confirmed by analytical chiral HPLC. Di-(*R*,*R*)-1-[10-(1-hydroxy-2,2,2-trifluoroethyl)-9-anthril]-2,2,2-trifluoroethyl muconate **2** was obtained in a 62% yield by esterifying *R*,*R*-ABTE with muconic acid at room temperature, in the presence of DCC and DMAP. (*S*,*S*,*S*,*S*)-**2** can be obtained by an analogous procedure from *S*,*S*-ABTE (Scheme 1).

The ^{1}H NMR spectrum of (*R*,*R*,*R*,*R*)-**2** at room temperature shows slow rotation around the sp^2-sp^3 (C_9-C_{11} and $C_{10}-C_{12}$) bonds resulting in broad resonances of protons H_1, H_2, H_3, H_4, H_5, H_6, H_7, and H_8, as has been observed already for other anthracenylalkylcarbinols such as ABTE.[8,12]

Taking into consideration that the main conformation of the benzylic bond keeps the C−CF_3 bond in a perpendicular position with respect to the anthracene plane, two low energy conformations for each substituted anthracenic group are possible. In one case, both CF_3 groups are placed on the same face of the anthracene (cisoid conformation), and in the other they are on opposite faces (transoid conformation). Considering that each molecule has two anthracenic groups, three different conformers are possible: cisoid-cisoid, transoid-cisoid, and transoid-transoid (Figure 1).

At low temperatures the internal rotation is frozen, and the relative conformations transoid and cisoid can be distinguished and assigned at the proton NMR spectrum (Figure 2) by using

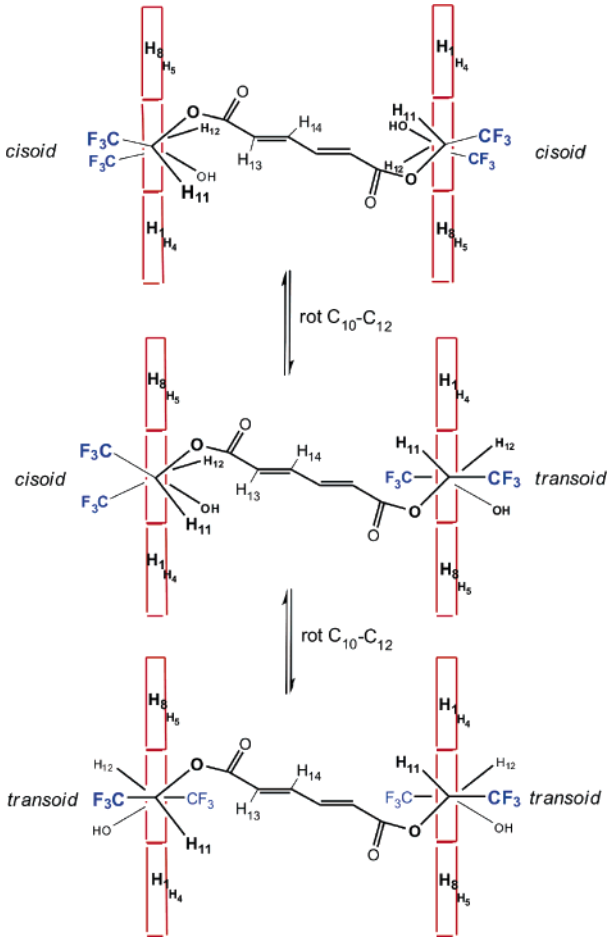

FIGURE 1. Vertical vision of the three rotamers of (*R*,*R*,*R*,*R*)-**2**.

(8) Pomares, M.; Sánchez-Ferrando, F.; Virgili, A.; Alvarez-Larena, A.; Piniella, J. F. *J. Org. Chem.* **2002**, *67*, 753−758.
(9) Estivill, C.; Pomares, M.; Kotev, M.; Ivanov, P.; Virgili, A.. *Tetrahedron: Asymmetry* **2005**, *16*, 2993−2997.
(10) (a) Endo, T.; Iida, T.; Furuya, N.; Yamada, Y.; Ito, M. M. *J. Chem. Software* **1999**, *5*, 82−92 (b) Klarner F. G.; Lobert M.; Naatz U.; Bandmann H.; Boese R. *Chem.—Eur. J.* **2003**, *9*, 5036−5047.
(11) Estivill, C.; Ivanov, P. M.; Pomares, M.; Sánchez-Arís, M.; Virgili. A. *Tetrahedron Asymmetry* **2004**, *15*, 1431−1436.

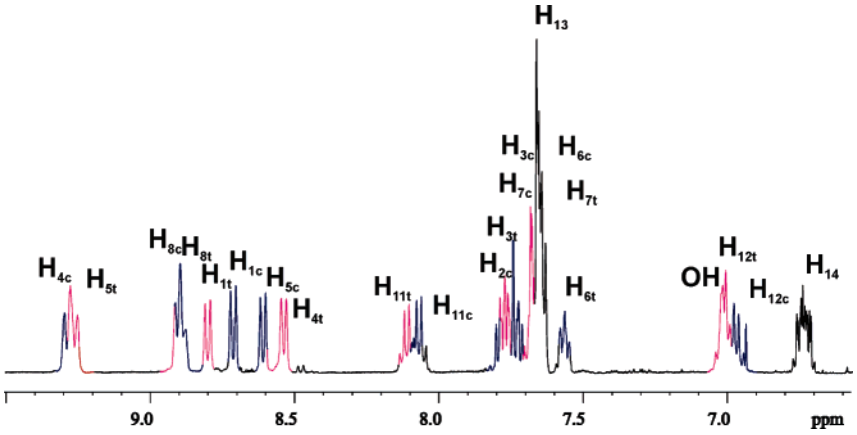

FIGURE 2. ^{1}H NMR spectrum of (*R*,*R*,*R*,*R*)-**2** in acetone-d_6 at 250 K (c: cisoid, t: transoid).

the information obtained from COSY and proton−carbon correlation spectra HSQC and HMQC (see Supporting Information).

The rotation barrier was measured by ^{1}H DNMR performed on the temperature dependence of protons H_1 and H_8 and protons H_4 and H_5. The Gibbs energy of the process was calculated using the Eyring equation obtaining a value of 14.5 kcal/mol (T_c = 320 K) for the $C_{10}-C_{12}$ bond, which is very similar to the barrier calculated for ABTE.[8] The value calculated for the C_9-C_{11} bond next to the ester group was slightly higher, 15.9 kcal/mol (T_c = 335 K), as this rotation is more sterically hindered. It is worth noting that compound **2** only shows signals in the aromatic region of the spectrum (6.5−9 ppm), leaving a large spectral window for substrate signals.

The conformational equilibrium and the C_2 symmetry of (*R*,*R*,*R*,*R*)-**2** made it impossible to obtain information about its global geometry using NMR cross-relaxation experiments. For this reason, we studied the conformational behavior of **2** with molecular mechanics (MacroModel package with MM3* force field).[13] Genetic algorithms, which were shown to be more effective than the Monte Carlo method, were used in order to explore the conformational space efficiently.[14] Four low energy conformations were found and two of them are arranged concavely: the anthracenic groups are in front of each other, perpendicular to the double bonds of the spacer molecule. The resulting clip like geometry seems to enhance the selective binding with aromatic guests (Figure 3).

Furthermore, diffusion of **2** was studied by DOSY techniques[15] obtaining at 295 K in $CDCl_3$ a diffusion coefficient of 8.25×10^{-5} cm^2/s at low concentrations (0−25 mM). At higher concentrations the coefficient decreases, resulting in 7.5×10^{-5} cm^2/s at 70 mM. The slower diffusion is due to self-association by compound **2**.

Chiral Induction Activity. The behavior of **2** as a chiral solvating agent was tested with several chiral substrates (Figure 4), all of which contained a hydrogen bond acceptor or donor

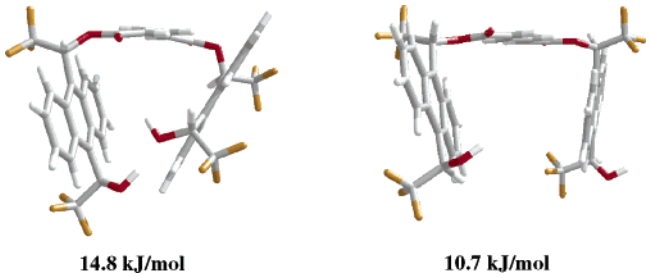

FIGURE 3. Low energy conformations of **2** with absolute energy values.

group and an aromatic group that allows π interaction. Enantiodifferentiation of phenylethanediol **3** and 1-(1-naphthyl)ethylamine **4** have already been studied with several other CSAs, so the discrimination achieved can be compared. The *cis*-1-amino-2-indanol **6** is a building block for several chiral compounds with applications in asymmetric synthesis and biologic systems.[16] Compounds **7** and **8** are the active principles of analgesics known as meptazinol[17] and piketoprofen.

In all cases, the experiments were carried out by adding portions of a CSA to a solution of racemic substrate (0.05 M) until a maximum increase of nonequivalence was obtained. The results obtained are summarized in Table 1. For all substrates, significant nonequivalences can be observed in several protons, which allow the enantiomeric relation[18] to be determined easily by integrating the separated signals. Separations of more than 0.2 ppm at room temperature are obtained for the protons H_9 and H_1 of compounds **4** and **5**. These are especially high if we take into account that the chiral auxiliary is only bound to the substrate through noncovalent forces. Figure 5 shows examples of the ^{1}H NMR spectra of some substrates, after CSA **2** is added. As illustrated, substrate signals move upfield because of the complexation effect.

If the temperature is decreased enantiodifferentiation increases, reaching almost 0.6 ppm for H_1 of **5**. The formation of diastereomeric complexes is thermodynamically favored and at low temperatures the contribution of the associated form to the averaged signal is higher.[3]

Nonequivalence could also be observed in the ^{13}C spectrum (Table 2 and Figure 6), which allows a better resolution to be

(12) Jaime, C.; Virgili, A.; Claramunt, R. M.; Lopez, C.; Elguero, J. *J. Org. Chem.* **1991**, *56*, 6521−6523.
(13) Mohamadi, F.; Richards, N. G. J.; Guida, W. C.; Liskam, R.; Lipton, M.; Caufield, C.; Chang, G.; Hendrickson, T.; Still, W. C. *J. Comput. Chem.* **1990**, *11* (4), 440−467.
(14) Nair, N.; Goodman, J. M. *J. Chem. Inf. Comput. Sci.* **1998**, *38*, 317−320.
(15) (a) Brand, T.; Cabrita, E. J.; Berger, S. *Prog. Nucl. Magn. Reson. Spectrosc.* **2005**, *46*, 159−196. (b) Esturau, N.; Sanchez-Ferrando, F.; Gavin, J. A.; Roumestand, C.; Delsuc, M.-A.; Parella, T. *J. Magn. Reson.* **2001**, *153*, 48−55. (c) Fielding, L. *Tetrahedron* **2000**, *56*, 6151−6170.
(16) Senanayake, C. H. *Aldrichimica Acta* **1998**, *31*, 3−15.
(17) Spiegel, K.; Pasternak, G. W. *J. Pharmacol. Exp. Ther.* **1984**, *228*, 414−419.
(18) Gawley, R. E. *J. Org. Chem.* **2006**, *71*, 2411−2416.

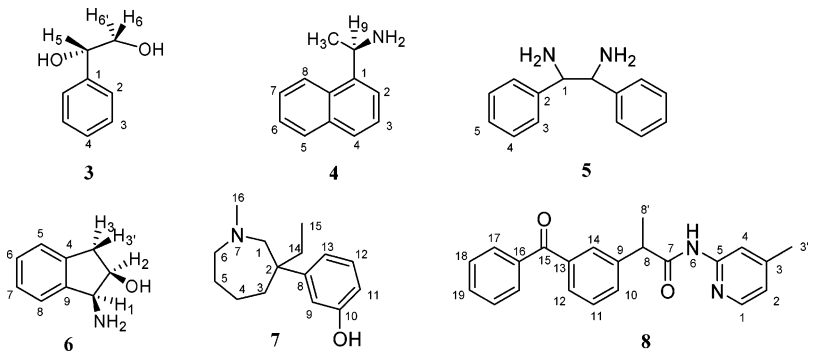

FIGURE 4. Chiral substrates evaluated in the enantiodiscrimination tests.

TABLE 1. Maximum Difference of the Enantiodistintion Δ(Δδ) of Several Signals of the ^{1}H NMR Spectrum between Enantiomers of 3−5 When (*R,R,R,R*)-2 Is Added

		Δ(Δδ) (ppm)	
substrate	proton	298 K	250 K
3	H_5	0.068	
	H_6	0.039	
	$H_{6'}$	0.039	
4	H_3	0.120	
	H_8	0.176	
	H_9	0.238	0.374
	H_{Me}	0.057	0.072
5	H_1	0.222	0.588
	H_3	0.045	
6	H_1	0.017	0.030
	H_2	0.012	0.013
	H_3	0.032	0.050
	$H_{3'}$	0.058	0.108
7	$H_{1'}$	0.035	0.036[a]
	H_1	0.053	0.080[a]
	H_3	0.148	
	H_{11}	0.021	0.030[a]
	H_{12}	0.017	0.039[a]
	H_{15}	0.091	
	H_{16}	0.040	0.066[a]
8	$H_{8'}$	0.086	0.158
	H_8	0.189	0.255
	H_1	0.031	

[a] 280 K.

obtained, especially of the aromatic zone. The high solubility of CSA **2** in nonpolar solvents, in contrast to other arylalkylcarbinols, is a significant advantage working with ^{13}C NMR or at low temperatures.

The enantiodiscrimination obtained for compounds **3** and **4** was compared with the nonequivalence observed for other, recently developed CSAs,[19] including CSA **1**, which is the starting compound of **2** achieving a higher enantiodiscrimination. Furthermore, a higher number of protons could be resolved. Table 3 shows the comparison with CSA **1**.[8] Moreover, the high solubility of **2** in nonpolar solvents increases its applicability.

Study of the Association Complexes. To understand why a higher enantiodiscrimination is obtained, the diastereomeric complexes of CSA with substrates **3** and **4** were studied in more detail. First, their stoichiometry was determined using Job's method,[20] obtaining a 1:1 composition for both cases.

The binding constants were measured using the equimolar method,[21] which is based on the variation of the chemical shift with the concentration, maintaining a 1:1 ratio between the CSA and the substrate. Under these conditions, the variation of $\Delta\delta$ analyzed as a function of $(\Delta\delta/S_0)^{1/2}$ (S_0 = concentration) results in a linear relation $[\Delta\delta = -(\delta_c/K)^{1/2}(\Delta\delta/S_0)^{1/2}]$ (δ_c = chemical shift of pure complex). We used pure enantiomers in separate experiments to detect differences between both diastereomeric complexes and avoid competitive processes. Tables 3 and 4 show the equilibrium constants obtained for the association of (*R*)-**3**, (*S*)-**3**, (*R*)-**4**, and (*S*)-**4** with (*R,R,R,R*)-**2** at different temperatures.Only a few differences between enantiomers can be observed. Furthermore, the values of *K* and ΔG energy are very similar to those obtained for (*R,R*)-**1**.

This allows us to conclude that the large enantiodifferentiation observed when (*R,R,R,R*)-**2** is used may be attributed to differences in the geometry of the complexes rather than to the thermodynamic factors. That is, because of the different relative positions of each enantiomer of the substrate associated with tweezer molecule **2**, the local magnetic fields induced by the π-system on several nuclei of each enantiomer must be really different. Moreover, the important differences obtained suggest that very close species are formed in which the influences are markedly increased.

To obtain information about their geometry, the diastereomeric complexes of (*R,R,R,R*)-**2** with amine **4** were studied with NOE spectra using gradient selection DPFGNOE[22] and 2D ROESY. When H_9 and CH_3 of the (*S*)-**4** were saturated, intermolecular NOE on H_{11} and H_1 of CSA **2** was obtained. These pairs of atoms should be close in space, assuming hydrogen bond interaction between the amine group and the hydroxyl group. The complex [(*R,R,R,R*)-**2** (*R*)-**4**] gave similar NOE results, which made it difficult to differentiate the complexes based on the NOE information.

The variation in the proton spectrum of CSA **2** at low temperatures after adding different amounts of (*R*)-**4** or (*S*)-**4** was also studied. Important and different changes in chemical

(19) (a) Iuliano, A.; Bartalucci, D.; Uccello-Barretta, G.; Balzano, F.; Salvadori, P. *Eur. J. Org. Chem.* **2001**, 2177−2184. (b) Nakatsuji, Y.; Nakahara, Y.; Muramatsu, A.; Kida, T.; Akashi, M. *Tetrahedron Lett.* **2005**, *46*, 4331−4335. (c) Dignam, C. F.; Zopf, J. J.; Richards, C. J.; Wenzel, T. J. *J. Org. Chem.* **2005**, *70*, 8071−8078. (d) Uccello-Barretta, G.; Iuliano, A.; Franchi, E.; Balzano, F.; Salvadori, P. *J. Org. Chem.* **1998**, *63*, 9197−9203. (c) Wilen, S. H.; Qi, J. Z.; Williard, P. G. *J. Org. Chem.* **1991**, *56*, 485−487. (d) Yanagihara, R.; Tominaga, M.; Aoyama, Y. *J. Org. Chem.* **1994**, *59*, 6865−6867.

(20) (a) Job, P. *Ann. Chem.* **1928**, *9*, 113−203.

(21) (a) Bouquant, J.; Chuche, J. *Tetrahedron Lett.* **1972**, *13*, 2337−2340. (b) Raber, D. J.; Hardee, L. E. *Org. Magn. Reson.* **1982**, *20*, 125−132.

(22) Stott, K.; Stonehouse, J.; Keeler, J.; Hwang, T.-L.; Shaka, A. J. *J. Am. Chem. Soc.* **1995**, *117*, 4199−4200.

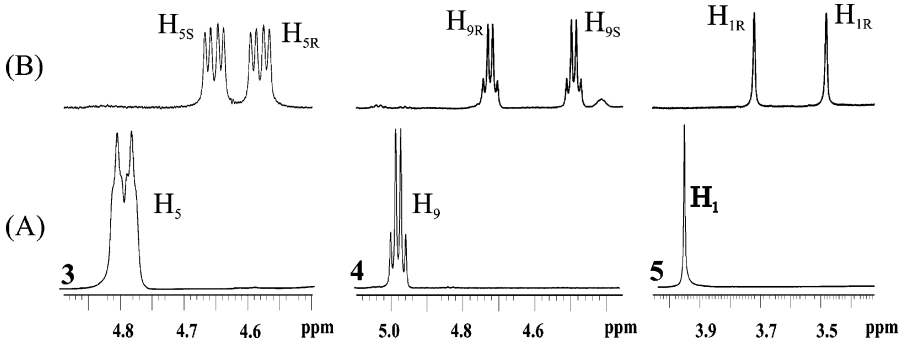

FIGURE 5. Enantiodifferentiation in the ^{1}H NMR spectra of substrates **3**, **4**, and **5** before (A) and after (B) adding 1−3 equiv of CSA **2**.

TABLE 2. Maximum Difference Δ(Δδ) in the ^{13}C NMR Spectrum Obtained for Substrates 3, 4, 5, 7, and 8 When (*R*,*R*,*R*,*R*)-2 Is Added

substrate	carbon	Δ(Δδ) (ppm)	carbon	Δ(Δδ) (ppm)
3	C_2	0.038	C_5	0.013
	C_7	0.023		
4	C_2	0.158	C_9	0.323
	C_3	0.076	C_{Me}	0.102
5	C_1	0.346	C_2	0.111
7	C_1	0.290	C_{12}	0.093
	C_3	0.382	C_{13}	0.029
	C_4	0.092	C_{14}	0.028
	C_9	0.028	C_{15}	0.082
8	C_1	0.032	C_{10}	0.022
	C_3	0.062	C_{11}	0.085
	C_5	0.053	C_{12}	0.130
	C_7	0.105	C_{13}	0.210
	C_8	0.105	C_{14}	0.130
	C_8'	0.082	C_{15}	0.056

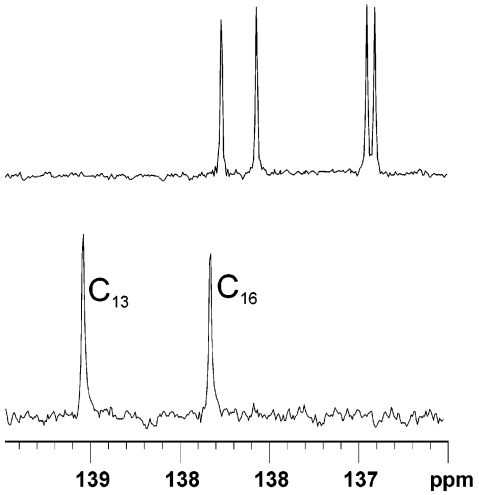

FIGURE 6. Enantiodifferentiation in the ^{13}C NMR spectrum of piketoprofen **8** after adding 3 equiv of CSA **2**.

shifts of protons of **2** were observed in both cases: while the signal at 9.08 (H_{4c}, H_{5t}) shifted upfield, the signals at 8.35 (H_{5c}, H_{4t}) and 6.7 (H_{12}) shifted downfield after complexion with the substrate (Figure 7). Moreover, the signal of protons H_{13} shifted downfield only in the case of the complex [(*R*,*R*,*R*,*R*)-**2** (*R*)-**4**].

The case for the proton H_{14} of the [(*R*,*R*,*R*,*R*)-**2** (*S*)-**4**] complex is particularly distinctive. The signal changes from a multiplet to four deformed doublets. It seems that the two H_{14} protons are no longer equivalent in the diastereometic complex, which

TABLE 3. Maximum Differences Δ(Δδ) in the ^{1}H NMR Spectrum Obtained between Enantiomers of 3−5 When (*R*,*R*,*R*,*R*)-2 or (*R*,*R*)-1 Is Added

		Δ(Δδ) (ppm)	
substrate	proton	(*R*,*R*,*R*,*R*)-**2**	(*R*,*R*)-**1**
3	H_5	0.068	0.021
	H_6	0.039	
	$H_{6'}$	0.039	
4	H_3	0.120	0.113
	H_8	0.176	0.119
	H_9	0.238	0.092
	H_{Me}	0.057	
6	H_1	0.027	0.026
	H_2	0.012	
	H_3	0.032	0.013
	$H_{3'}$	0.058	0.049

TABLE 4. Equilibrium Constants of the Complexes Formed between the Enantiomers of 3 with (*R*,*R*,*R*,*R*)-2, Measured Using the Equimolar Method

	(*R*)-**3**		(*S*)-**3**	
T (K)	K_R M^{-1}	ΔG°_R kJ/mol	K_S M^{-1}	ΔG°_S kJ/mol
295	7.1 (±0.3)	−4.8 (±0.1)	6.9 (±0.6)	−4.7 (±0.2)
275	8.2 (±0.7)	−4.8 (±0.2)	10 (±2)	−5.2 (±0.3)
250	35 (±4)	−7.4 (±0.2)	39 (±15)	−7.5 (±0.8)

TABLE 5. Equilibrium Constants of the Complexes Formed between the Enantiomers of 4 with (*R*,*R*,*R*,*R*)-2, Measured by the Equimolar Method

	(*R*)-**4**		(*S*)-**4**	
T (K)	K_R M^{-1}	ΔG°_R kJ/mol	K_S M^{-1}	ΔG°_S kJ/mol
295	28.0 (±6)	−8.14 (±0.5)	24.4 (±0.4)	−7.83 (±0.0.4)
275	49.9 (±0.5)	−9.60 (±0.03)	50.0 (±3)	−9.60 (±0.1)
250	90 (±10)	9.3 (±0.2)	91 (±5)	−11.1 (±0.1)

demonstrates that CSA **2** adopts a different, asymmetric conformation when it is associated with (*S*)-**4**. The flexibility of CSA **2** allows a conformational adaptation of the host molecule toward the guest molecule. In the case of the complex with (*R*)-**4**, the signal of the H_{14} protons remains similar to the noncomplexed form.

If we focus now on the substrate signals, we see that they all shifted upfield as expected. These shifts are different for each enantiomer, which is the base of the observed enantiodiscrimination. In the case of the enantiomer (*S*)-**4**, the protons H_2, H_8, H_9, and CH_3 are more affected by the formation of the complex, with chemical shift differences of 0.21, 0.41, 0.34, and 0.16

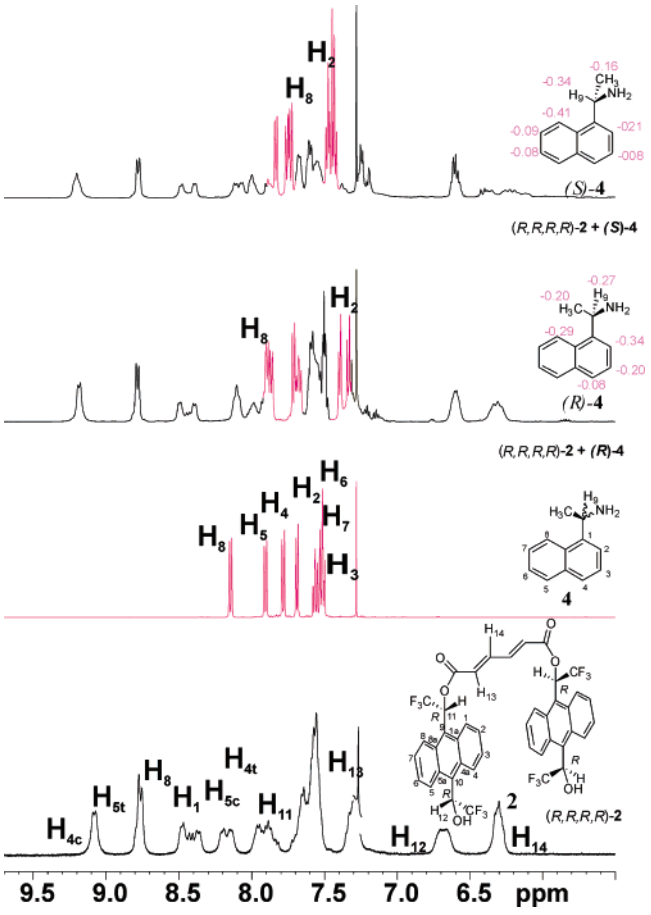

FIGURE 7. ^{1}H NMR spectra at 270 K of **4**, (*R*,*R*,*R*,*R*)-**2**, and equimolar mixtures of (*R*,*R*,*R*,*R*)-**2** and enantiomers (*R*)-**4** and (*S*)-**4**. The variation of the chemical shift is indicated in the side formulas.

ppm, than the uncomplexed form. For (*R*)-**4** we obtain chemical shift variations of 0.34, 0.29, 0.27, 0.20, and 0.20 for the protons H_2, H_8, H_9, CH_3, and H_3. Comparatively, protons H_8 and H_9 are the most strongly modified in the complex of (*S*)-**4**, and H_2, H_3, and CH_3 are the most shifted in the complex of (*R*)-4. Assuming that the deeper the penetration is, the higher the magnetic influence, a conclusion can be drawn from the differences observed in the averaged orientation of amine **4** in the cavity determined by the CSA. In the case of (*S*)-**4**, the substrate introduces itself in the chiral cavity with the H_8H_9-side first, while for (*R*)-**4** the H_2H_3-side enters the molecular receptor first.

Conclusions

The results obtained in this work allow us to conclude that **2** is an excellent CSA. It improves the enantiodiscrimination obtained until now with other recently developed CSAs and allows the enantiomeric purity of different active principles to be determined. No thermodynamic differences between the diastereomeric complexes were found. For 1-(1-naphthyl)-ethylamine, a different geometry of these was established by different changes in the chemical shift of the CSA and of the substrate after association. It seems that the conformational adaptation of **2** allows the CSA to optimize its geometry to form the most favorable complex, which is different for each enantiomer.

Experimental Section

Theoretical Calculations. The conformational search was carried out with the genetic algorithm GACK, which can be downloaded from the Cambridge Chemistry Department www server on URL: http: //www.ch.cam.ac.uk/. This program works in tandem with MacroModel, which handles the structural minimization using the MM3* force field, in our case. The poolsize and the number of generations are important parameters. These were both set to 32, obtaining 1240 final structures, of which 382 were different. The cross over rate was set to 1.0 and the mutation rate per molecule to 0.4. Selection and replacement temperature were 10000 and 1000 K, respectively. The conformational search was repeated five times with different input structures, obtaining equivalent results in all cases. NMR spectra were recorded at 400 and 500 MHz for 1 h. The temperature was controlled to 0.1 °C. The NMR signals were identified completely with the aid of several 1D (NOE) and 2D (COSY, NOESY, HMQC, and HMB) spectra. Diffusion experiments were recorded using ledbpgp2s sequence from Bruker Topspin Library.

The NMR titration method was carried out with 0.4−0.5 mL of a solution 0.03−0.05 M of the compound (**3**−**8**) with several portions of 0.2−0.5 equiv of CSA **2** added. The NMR spectrum was measured after each addition, and the variation of the chemical shift was calculated. The measurements where made until maximum enantiodiscrimination was reached.

Binding constants were determined using the equimolar method, measuring the chemical shifts of an equimolar solution in $CDCl_3$ of the substrate (**3** or **4**) and the CSA. Five portions of 0.1 mL were added to 0.4 mL of an initial concentration of 0.05 M, and the chemical shift was measured. The process was repeated for different temperatures.

Synthesis of Di-(*R*,*R*)-1-[10-(1-hidroxy-2,2,2-trifluoroethyl)-9-anthryl]-2,2,2-trifluoroethyl muconate 2. Muconic acid (185 mg, 1.3 mmol) was added to a solution of (*R*,*R*)-α,α′-(bistrifluoromethyl)-9,10-anthracenedimethanol **1** (1.00 g, 2.6 mmol), DCC (1.070 g, 5.2 mmol), and DMAP (96 mg, 0.79 mmol) in anhydrous CH_2Cl_2 (150 mL) under nitrogen. The reaction mixture was stirred for 4 h at ambient temperature and then treated with 1 M HCl (120 mL), 1 M $NaHCO_3$ (120 mL), and a saturated solution of NaCl (120 mL). The organic phase was dried over $MgSO_4$, and the volatiles where removed under reduced pressure. Purification of the product using silica gel flash chromatography (eluent EtOAc/hexane, 10:1) gave diester (*R*,*R*,*R*,*R*)-**2** (707 mg, 62%) as a yellow solid: mp 177−178 °C; $[\alpha]^{20}_D$ +177 (*c* 1.0, $CHCl_3$). ^{1}H NMR (500 MHz, acetone-d_6, 250 K): δ (*cisoid*) 9.29 (d, J = 9 Hz, 1H, H_4), 8.91 (d, J = 9 Hz, 1H, H_8), 8.72 (d, J = 9 Hz, 1H, H_1), 8.54 (d, J = 9 Hz, 1H, H_5), 8.07 (q, J = 8 Hz, 1H, H_{11}), 7.84 (dd, J = 9 Hz, J = 9 Hz, 1H, H_2), 7.76 (dd, J = 9 Hz, J = 9 Hz, 1H, H_7), 7.66 (m, 3H, H_3 and H_{13}), 7.65 (dd, J = 9 Hz, J = 9 Hz, 1H, H_6), 7.58 (dd, J = 9 Hz, J = 9 Hz, 1H, H_3), 7.01 (m, 2H, H_{OH}), 6.98 (m, 2H, H_{12}), 6.75 (m, 2H, H_{14}); (*transoid*) 9.26, J = 9 Hz, 1H, H_5), 8.89 (d, J = 8 Hz, 1H, H_8), 8.81 (d, J = 9 Hz, 1H, H_1), 8.62 (d, J_t = 9 Hz, 1H, H_4), 8.12 (q, J = 8 Hz, 1H, H_{11}), 7.79 (dd, J = 9 Hz, J = 9 Hz, 1H, H_2), 7.78 (dd, J = 9 Hz, J = 9 Hz, 1H, H_3), 7.69 (dd, J = 9 Hz, J = 8 Hz, 1H, H_7), 7.66 (m, 3H, H_{13}), 7.58 (dd, J = 9 Hz, J = 9 Hz, 1H, H_6), 7.01 (m, 2H, H_{OH}), 6.98 (m, 2H, H_{12}), 6.75 (m, 2H, H_{14}). ^{13}C NMR (500 MHz, acetone-d_6, 250 K): δ (*cisoid*) 163.7 (C_{12}), 143.9 (C_{13}), 132.3 (C_{4a}), 131.7, 131.5 (C_{8a}, C_{1a}), 130.3 (C_{5a}), 129.0 (CF_3), 130.3 (C_4), 128.2 (C_{14}), 127.8 (C_3), 127.3 (C_8), 126.8 (C_5), 125.6 (C_1), 124.6 ($C_{1'c}$), 123.8 (C_{1c}); (*transoid*) 163.7 (C_{12}), 143.9 (C_{13}), 131.4, 131.3, 131.1, 130.9 (C_{5a}, C_{8a}, C_{1a}, C_{4a}), 129.0 (CF_3), 129.5 (C_5), 128.2 (C_{14}), 128.3 (C_1), 127.4 (C_3), 127.4 (C_4), 126.7 (C_8), 124.5 (C_6), 124.8 (C_1). HRMS (ESI$^-$): *m*/*z* 853.1474 (M^-, δ −2.08 ppm).

Acknowledgment. Financial support from CYCYT (Grant PPQ2000-0369 and Grant BQU2003-01231) and a predoctoral grant (FPU) from the Ministerio de Educación y Ciencia de

España are gratefully acknowledged. The Servei de Ressonància Mangnètica Nuclear of the UAB is also acknowledged for allocating instrument time.

Supporting Information Available: Characterization data of compound **2** (NOE, 2D NOESY, COSY, ^{13}C NMR, HSQC, HMBC, ^{1}H DNMR complete line shape analysis, high-resolution mass spectrum), computational data, enantiodiscrimination spectra with compounds **3**−**8**, Job plots, plots of equimolar method calculations, intermolecular NOE spectra, as well as ^{1}H NMR titration of compound **2** with substrate **4**. This material is available free of charge via the Internet at http://pubs.acs.org.

JO061276D